



Sensitive and Multiplexed On-chip microRNA Profiling in Oil-Isolated Hydrogel Chambers**

Hyewon Lee, Rathi L. Srinivas, Ankur Gupta, and Patrick S. Doyle*

Abstract: Although microRNAs (miRNAs) have been shown to be excellent indicators of disease state, current profiling platforms are insufficient for clinical translation. Here, we demonstrate a versatile hydrogel-based microfluidic approach and novel amplification scheme for entirely on-chip, sensitive, and highly specific miRNA detection without the risk of sequence bias. A simulation-driven approach is used to engineer the hydrogel geometry and the gel-reaction environment is chemically optimized for robust detection performance. The assay provides 22.6 fM sensitivity over a three log range, demonstrates multiplexing across at least four targets, and requires just 10.3 ng of total RNA input in a 2 hour and 15 minutes assay.

MicroRNAs (miRNAs) are short noncoding RNAs that have recently emerged as promising diagnostic markers for several diseases because of their high stability and unique dysregulation patterns.^[1] However, clinical translation of miRNA diagnostics still faces several practical challenges.^[1c,2] These include sequence homology, diversity of abundance, and the exacting demands of a clinical assay, which requires multiplexed, sensitive, and specific analysis of small panels of miRNAs from low sample inputs while minimizing assay time, external equipment and number of cumbersome steps.^[2b,3] While northern blotting is still widely used for its specificity, the need for large RNA input (5–25 µg), long processing time, and low sensitivity (in the nM range) render it infeasible for clinical application.^[4] Although other commercial platforms provide large multiplexes and higher sensitivity, they still fall short on the other metrics.^[5] Microarray assays require overnight hybridization, several steps, and complicated equipment for fluid control.^[2b] Meanwhile, quantitative real-time polymerase chain reaction (qPCR) based methods are at risk of sequence bias arising from target-based amplification and can require a large (> 500 ng) amount of input RNA.^[2b,5a] Commercial microfluidic versions of qPCR reduce assay volume and improve throughput, but still require cDNA synthesis prior to chip-loading, and use target amplification.^[6]

Furthermore, studies that have compared commercial profiling methods have found inter-platform discrepancies in miRNA quantification.^[7] Recently developed microfluidic on-chip assays or lateral flow assays have been able to decrease assay time, making systems suitable for point-of-care testing but do not meet all other clinical needs.^[8] A recent study used isotachopheresis for rapid and specific let-7a detection from total RNA samples, but the system could not multiplex, offered only moderate detection sensitivity (10 pM), and required extensive optimization for specificity. Besides, fluidic limitations demanded a much larger quantity of total RNA (1 µg) than was actually processed through the device (5 ng).^[8d] Another recent study demonstrated a power-free PDMS chip for miRNA quantification in resource-limited settings with better sensitivity (500 fM) over short (20 minutes) times, but did not make multiplexed measurements from patient samples.^[8a,b,c] Our approach addresses the limitations of these prior works.

Our group has previously shown the superiority of non-fouling polyethylene glycol (PEG) hydrogel microparticles in comparison to surface-based systems for multiplexed miRNA detection.^[9] Hybridization kinetics and reaction thermodynamics are both more favorable in a hydrogel, leading to better sensitivity and specificity.^[10] Our gel-particle-based approach, had also included development of a unique universal labeling scheme, eliminating the need to tailor labels on a target-by-target basis and minimizing the possibility of sequence bias, such as in qPCR. Now, we develop an entirely on-chip miRNA assay which takes advantage these hydrogel-specific detection advantages and adopts our labeling scheme while leveraging the precise fluidic control inside a microfluidic channel. We further optimize and adapt a novel amplification scheme that we recently developed^[11] to achieve high sensitivity and minimize total RNA input for multiplexed measurements.

miRNA probe functionalized hydrogel posts were immobilized in reusable glass channels using projection lithography,^[12] which provided precise control over shape and size of the gel scaffolds. Multiplexing was achieved through a spatial encoding scheme as described in previous work^[11] and as shown in Figure 4b for three miRNA targets. Posts bearing different probes were fabricated through sequential rounds of polymerization (see the Supporting Information). The probe DNA had two regions: a miRNA target-binding domain and a universal linker domain used for labeling (Figure 1a). After 90 min miRNA hybridization, a biotinylated universal linker was ligated to the probe–target complex (10 minutes), and the complex was finally labeled using a streptavidin-conjugated fluorophore (SA-PE, 30 minutes) or using a streptavidin-conjugated enzyme (SAB, 15 minutes). In the latter case,

[*] Dr. H. Lee,^[†] R. L. Srinivas,^[†] A. Gupta, Prof. P. S. Doyle
Department of Chemical Engineering
Massachusetts Institute of Technology
77 Massachusetts Avenue, Cambridge, MA 02139 (USA)
E-mail: pdoyle@mit.edu

[†] These authors contributed equally to this work.

[**] We acknowledge support from the NIH Center for Future Technologies in Cancer Care U54-EB-015403-01, the NCI grant 5R21A177393-02, Eni S.p.A. and NSF grant CMI-1120724.

Supporting information for this article is available on the WWW under <http://dx.doi.org/10.1002/anie.201409489>.

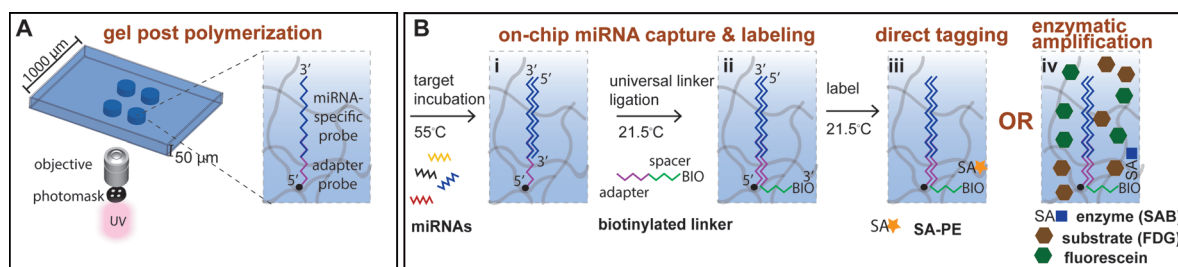


Figure 1. Post polymerization and miRNA assay scheme. A) Posts are polymerized using projection lithography. Probes functionalized inside gel posts are engineered with two domains: a miRNA-binding domain and a universal linker domain. B) The target is incubated on a hot plate and subsequently ligated to the biotinylated linker and labeled using either the streptavidin-conjugated fluorophore (SA-PE) or streptavidin-conjugated enzyme (SAB) amplification scheme.

there was an additional amplification step (15 minutes) that occurred in the confined environment of the hydrogel (Figure 1b). All assay steps used a steady, high Péclet number gravity-driven flow, eliminating the use of expensive flow controllers while maintaining constant reagent delivery in the channel. Steps requiring heating or cooling were performed on a hot plate, enabling stable and continuous sample delivery without need for sample pre-heating (see the Supporting Information).

The first clinically relevant miRNA target considered in this study was let-7a, which is dysregulated in several cancers^[13] but has high sequence homology with other let-7 family members (Figure 2). Let-7 is thus widely regarded as a particularly difficult miRNA family to detect specifically. Using our unique gel environment and universal labeling scheme, we sought to achieve robust let-7 sequence discrimination by tuning incubation conditions rather than by custom-engineering probe designs as in other studies.^[8d,14] It is well known that miRNAs vary widely in terms of melting temperatures (T_m) and that imposing stringency to benefit specificity of one target could severely affect sensitivity of another; it was thus important to find incubation conditions that would provide specificity while accommodating multiplexing of small panels of miRNAs. Indeed, systems that process hundreds or thousands of miRNA targets such as microarrays have been extensively engineered to provide optimal results across all targets being measured but still struggle with discrimination between let-7 variants with cross-reactivities as high as 50%.^[5a,15] Meanwhile for some research platforms, attaining specific miRNA detection (< 15% cross

reactivity) has required complicated and customized probe designs for each miRNA target.^[8d,16] Here, it was postulated that higher association constants for nucleic acid binding in the gel environment relative to a surface^[17] would enable imposition of stringent incubation conditions for specificity without precluding high sensitive detection. Indeed, high specificities were achieved (maximum cross reactivity of 11.3%) by simply tuning salt concentration of the hybridization buffer (250 mM NaCl), probe concentration (5 μ M inside gel) and by using a high (55°C) assay temperature, which was chosen based on sequence T_m (Figure 2, see the Supporting Information). Additionally, in a real clinical setting where necessary, it should be possible to account for the cross-reactivities reported here by polymerizing additional sets gel posts bearing probes for relevant variants of the sequence (see the Supporting Information). Notably, there was no need for expensive locked nucleic acid (LNA) probes to achieve this specificity although future iterations using such T_m optimized probes may lead to even better results. Furthermore, since the platform is primarily intended for measurement of small panels of miRNAs, specificity and sensitivity can be attained for all targets by simply tuning probe concentrations in the gel (see the Supporting Information). Using SA-PE, our assay conditions provided specific and measurable signal at 10 pM target (see the Supporting Information), but best performance in the stringent incubation conditions was achieved through integration and rational optimization of a novel amplification scheme that we previously developed for DNA detection in PDMS devices.^[11] In the scheme, after gel-bound complexes are labeled with SAB, the channel is flushed with enzymatic substrate (FDG) and subsequently with fluorinated oil (FC-40). The latter step confines the gel posts within the oil phase and traps FDG due to high hydrodynamic resistance inside the gel post relative to the surrounding channel. Enzymatically turned over fluorescent reaction products are then dramatically concentrated in the now confined compartments (Figure 3a), leading to large signal boosts in short (15 minutes) amplification times.

To translate our scheme into the hydrophilic glass microchannels, it was first necessary to design a hydrogel geometry that would lead to optimal oil encapsulation, structural stability under flow, and minimization of diffusional limitations. The latter two parameters were determined based on experimental observation and provided us with minimum

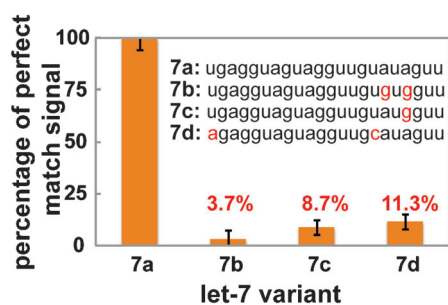


Figure 2. Let-7a detection specificity using 250 mM NaCl in hybridization buffer. The maximum observed cross reactivity is 11.3%.

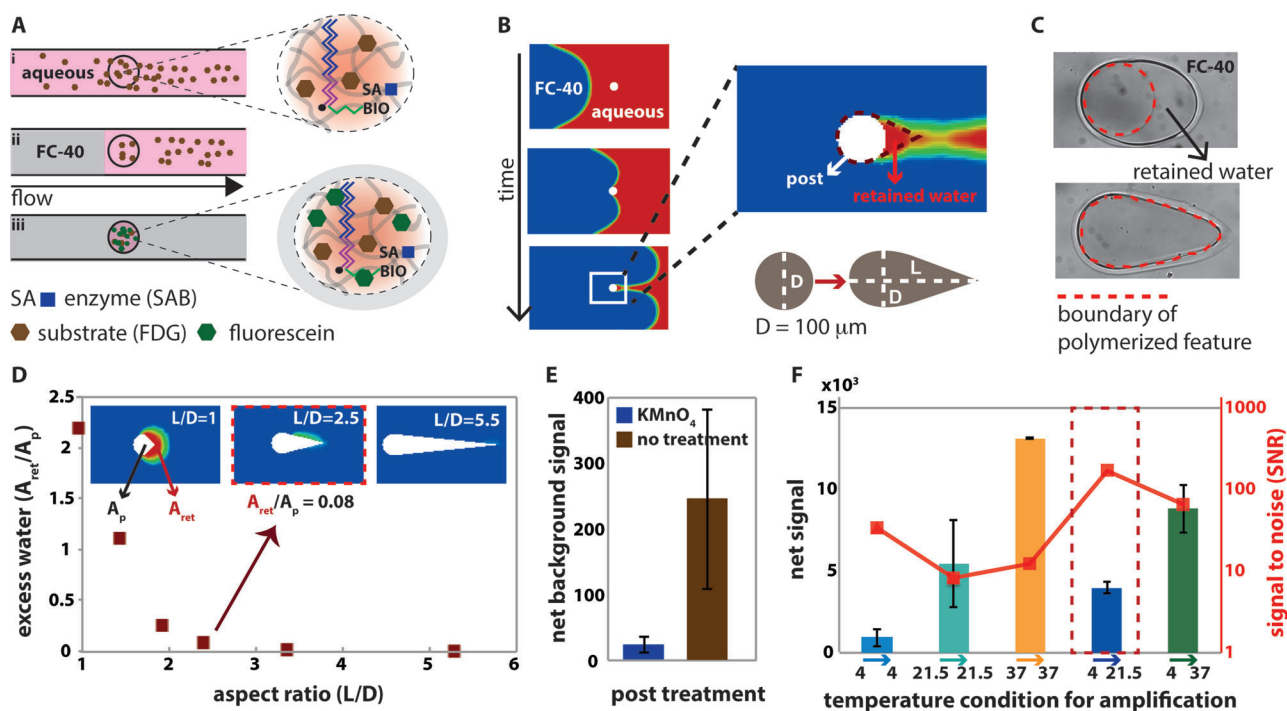


Figure 3. Oil isolation and amplification optimization. A) The channel is i) filled with substrate, ii) flushed with FC-40, and iii) posts are isolated within the oil phase allowing amplification to occur in the confined gel environment. B) Simulation results of a two phase flow around a cylindrical post in a microchannel showing the tendency of water to attach in a raindrop shape. C) Experimental results demonstrating the superiority of a raindrop shape over a cylindrical shape for encapsulation and minimization of reentrained water. D) Simulation results showing that L/D is the main parameter that determines excess water retained around post. E) Experimental results showing that KMnO_4 treatment reduces nonspecific signal on a post. F) Temperature optimization of the amplification step. An initial cooling step followed by a ramp up to 21.5 °C gives the best SNR.

(100 μm) and maximum (300 μm) width dimensions for our posts respectively (see the Supporting Information). Even in our previous study, which had used hydrophobic PDMS-channels, it was noticed that a cylindrical geometry was suboptimal for oil-encapsulation, since there was occasional uneven entrainment of water around the posts during the oil flush. This could possibly affect reagent concentrations from post to post. The problem was further exaggerated in the hydrophilic glass channels, likely due to different contact angles of the oil with the channel walls. A better hydrogel shape was thus rationally engineered by computationally modeling a two-phase flow around a post in a hydrophilic channel.

From simulations, it was immediately apparent that water pinches off from the edge of the cylindrical post in a “raindrop” shape that may be a better geometric design for the gel (Figure 3b). This hypothesis was experimentally confirmed (Figure 3c) and further simulations were performed to optimize dimensions. The key parameter that determined water entrainment fraction around the post was found to be ratio of the length of the post (L) to its diameter (D). As L/D increases, there is better encapsulation. From a practical standpoint though, increasing post length decreased channel space for multiplexing. Considering this trade off, we proceeded using $L/D = 2.5$ for all ensuing studies, since there was minimal benefit in increasing it further (Figure 3d, see the Supporting Information for simulation details).

From a chemical standpoint, the aim was to minimize assay time while maximizing signal-to-noise ratios (SNRs) by adjusting the gel environment. For example, overcoming kinetic barriers in short (15 minutes) enzyme incubations required use of SAB at high ($1 \text{ ng}\mu\text{l}^{-1}$) concentration, but there was a tendency for collection of high nonspecific signal at these conditions (Figure 3e). It was hypothesized that this could be due to relative hydrophobicity of the hydrogel, which likely has double bonds from unconverted acrylate groups during the polymerization process.^[18] We thus used a chemical (KMnO_4) that oxidized these double bonds^[19] and made the gel more hydrophilic (see the Supporting Information for FTIR data). Indeed, we found that the KMnO_4 treatment drastically decreased nonspecific signal (Figure 3e). Next, the impact of amplification temperature was explored since SAB has demonstrated temperature dependence in previous studies.^[20] Interestingly, at low temperatures (4 °C) the enzymatic reaction was almost entirely arrested whereas at increased temperatures (21.5, 37 °C), there was significantly higher signal but lower SNRs. Ultimately, optimal results and highest SNRs were gained by combining low temperature and high temperature conditions: the chip was cooled to 4 °C for the substrate/oil flush, which we hypothesize enabled more uniform substrate loading, and was then brought to 21.5 °C for the remainder of the reaction (Figure 3f). Together, optimization of gel chemistry and amplification temperature significantly reduced incubation

times relative to our previous work (30 minutes here vs. 80 minutes before^[11]) while still achieving high sensitivity without post-to-post cross-talk. Furthermore, this optimized scheme eliminated any need for channel surface treatments such as fluorination, which often deposit nonuniformly and makes channel cleaning difficult (see the Supporting Information). The assay now demonstrated a let-7a detection limit of 22.6 fM (see the Supporting Information), which is over one order of magnitude better than previously mentioned competing on-chip assays.^[8a,d] In the future, it may be possible to gain even better sensitivity by integrating LNA probes, which should be straightforward and compatible with our flexible synthesis and assay approach.

For miRNA diagnostic assays though, sensitivity is most relevant in the context of total input RNA required for quantification. We thus sought to minimize total RNA consumption over the hybridization time scale (90 minutes) used while ensuring constant delivery to the posts. This input requirement can in fact be drastically reduced by further controlling flow conditions or by running the hybridization for shorter times, which is still expected to give significant signal (see the Supporting Information). Consistent flow delivery was confirmed by measuring signal from 10 pM of a synthetic RNA sequence (miSpike) in all channels. Let-7a was first measured in a representative lung tumor total RNA sample using both SA-PE and the amplification scheme to characterize amount of required input material with both schemes; using the SA-PE scheme, we needed 172 ng RNA, but with the amplification scheme, this was reduced to just 10.3 ng, indicating an about 17-times increase in limit of detection over the same assay time and need for over 400-fold less total RNA than northern blotting (Figure 4a). By further controlling flow conditions, it is expected that required input RNA could be as low as 15–200 pg (see the Supporting Information).

This initial characterization enabled multiplexed measurements for three miRNA targets (see the Supporting Information) and comparison of miRNA expression in tumor versus healthy tissue using our on-chip assay. All of the dysregulation patterns reported here are expected according to literature,^[9b,13b,21] and it was possible to use 10X lower input RNA (50 ng) with our enzymatic amplification scheme relative to the direct labeling scheme (500 ng) to achieve the same results (Figure 4b). These results were further validated using our previously published gel particle assay (Figure 4b), which itself had previously displayed excellent agreement with qPCR. Importantly, the new enzymatic amplification scheme was able to provide quantitative and multiplexed miRNA profiling results in an entirely on-chip assay using low amounts of total RNA without adding additional assay time, and has the flexibility to be performed over even shorter time scales.

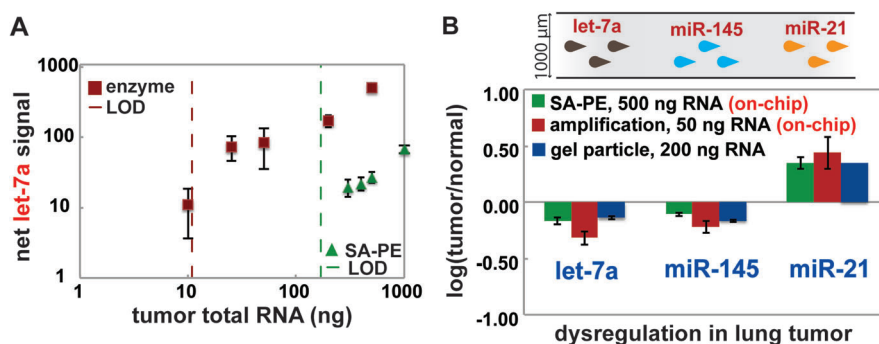


Figure 4. miRNA quantification from total RNA. A) Using SA-PE requires 172 ng total RNA whereas the amplification scheme brings input requirement down to 10.3 ng for let-7a quantification. B) Demonstration of the multiplexing scheme and measurement of dysregulation ratios of three miRNAs in healthy versus tumor tissues and demonstration of ability to measure using less total RNA when employing the enzymatic amplification. Results are validated using previously published gel particle results.^[9b]

In summary, the hydrogel-based on-chip assay and enzymatic amplification scheme shown here is specific, sensitive, and highly tunable depending on clinical needs and does not require extensive modification based on target. Our system provides at least one order of magnitude better sensitivity than competing on-chip assays while allowing multiplexing, and quantification of miRNAs from low amounts (about 10.3 ng) of total RNA sample was demonstrated without introducing sequence bias. We fully expect that with optimized flow control this input amount can be even further reduced (see the Supporting Information) and that the versatile system shown here shows great promise for sensitive and multiplexed miRNA detection.

Received: September 25, 2014

Revised: November 10, 2014

Published online: January 7, 2015

Keywords: amplification · diagnostics · hydrogels · microfluidics

- [1] a) G. A. Calin, C. M. Croce, *Nat. Rev. Cancer* **2006**, *6*, 857–866; b) T. Y. Ha, *Immune Netw.* **2011**, *11*, 135–154; c) C. C. Pritchard, H. H. Cheng, M. Tewari, *Nat. Rev. Genet.* **2012**, *13*, 358–369; d) K. U. Tüfekci, M. G. Oner, R. L. J. Meuwissen, S. Genc, *Methods Mol. Biol.* **2014**, *1107*, 33–50.
- [2] a) M. Baker, *Nat. Methods* **2010**, *7*, 687–692; b) P. Chugh, D. P. Dittmer, *Wiley Interdiscip. Rev. RNA* **2012**, *3*, 601–616.
- [3] S. Lingam, M. Beta, D. Dendukuri, S. Krishnakumar, *MicroRNA* **2014**, *3*, 18–28.
- [4] a) M. de Planell-Saguer, M. C. Rodicio, *Anal. Chim. Acta* **2011**, *699*, 134–152; b) J. Koshiol, E. Wang, Y. Zhao, F. Marincola, M. T. Landi, *Cancer Epidemiol. Biomarkers Prev.* **2010**, *19*, 907–911.
- [5] a) P. Mestdagh, N. Hartmann, L. Baeriswyl, et al., *Nat. Methods* **2014**, *11*, 809–815; b) V. Del Vecovo, T. Meier, A. Inga, M. A. Denti, J. Borlak, *Plos One* **2013**, *8*, e78870.
- [6] a) F. Moltzahn, A. B. Olshen, L. Baehner, et al., *Cancer Res.* **2011**, *71*, 550–560; b) J. S. Jang, V. A. Simon, R. M. Feddersen, F. Rakhshan, D. A. Schultz, M. A. Zschunke, W. L. Lingle, C. P. Kolbert, J. Jen, *BMC Genomics* **2011**, *12*, 144.
- [7] B. Wang, P. Howel, S. Bruheim, J. F. Ju, L. B. Owen, O. Fodstad, Y. G. Xi, *Plos One* **2011**, *6*, 0.

- [8] a) H. Arata, H. Komatsu, A. S. Han, K. Hosokawa, M. Maeda, *Analyst* **2012**, *137*, 3234–3237; b) H. Arata, H. Komatsu, K. Hosokawa, M. Maeda, *Plos One* **2012**, *7*, e48329; c) G. Garcia-Schwarz, J. G. Santiago, *Anal. Chem.* **2012**, *84*, 6366–6369; d) G. Garcia-Schwarz, J. G. Santiago, *Angew. Chem. Int. Ed.* **2013**, *52*, 11534–11537; *Angew. Chem.* **2013**, *125*, 11748–11751; e) H. Arata, K. Hosokawa, M. Maeda, *Anal. Sci.* **2014**, *30*, 129–135; f) X. F. Gao, H. Xu, M. Baloda, A. S. Gurung, L. P. Xu, T. Wang, X. J. Zhang, G. D. Liu, *Biosens. Bioelectron.* **2014**, *54*, 578–584.
- [9] a) S. C. Chapin, P. S. Doyle, *Anal. Chem.* **2011**, *83*, 7179–7185; b) S. C. Chapin, D. C. Appleyard, D. C. Pregibon, P. S. Doyle, *Angew. Chem. Int. Ed.* **2011**, *50*, 2289–2293; *Angew. Chem.* **2011**, *123*, 2337–2341.
- [10] D. C. Pregibon, P. S. Doyle, *Anal. Chem.* **2009**, *81*, 4873–4881.
- [11] R. L. Srinivas, S. D. Johnson, P. S. Doyle, *Anal. Chem.* **2013**, *85*, 12099–12107.
- [12] J. C. Love, D. B. Wolfe, H. O. Jacobs, G. M. Whitesides, *Langmuir* **2001**, *17*, 6005–6012.
- [13] a) H. H. Zhang, X. J. Wang, G. X. Li, E. Yang, N. M. Yang, *World J. Gastroenterol.* **2007**, *13*, 2883–2888; b) J. Takamizawa, H. Konishi, K. Yanagisawa, S. Tomida, H. Osada, H. Endoh, T. Harano, Y. Yatabe, M. Nagino, Y. Nimura, T. Mitsudomi, T. Takahashi, *Cancer Res.* **2004**, *64*, 3753–3756.
- [14] a) J. Q. Yin, R. C. Zhao, K. V. Morris, *Trends Biotechnol.* **2008**, *26*, 70–76; b) C. G. Liu, G. A. Calin, S. Volinia, C. M. Croce, *Nat. Protoc.* **2008**, *3*, 563–578.
- [15] H. Wang, R. A. Ach, B. Curry, *RNA* **2007**, *13*, 151–159.
- [16] J. M. Lee, Y. Jung, *Angew. Chem. Int. Ed.* **2011**, *50*, 12487–12490; *Angew. Chem.* **2011**, *123*, 12695–12698.
- [17] N. V. Sorokin, V. R. Chechetkin, S. V. Pan'kov, O. G. Somova, M. A. Livshits, M. Y. Donnikov, A. Y. Turygin, V. E. Barsky, A. S. Zasedatelev, *J. Biomol. Struct. Dyn.* **2006**, *24*, 57–66.
- [18] E. Andrzejewska, *Prog. Polym. Sci.* **2001**, *26*, 605–665.
- [19] J. McMurry, *Organic chemistry*, 6th ed., Thomson-Brooks/Cole, Belmont, CA, **2004**.
- [20] T. G. Park, A. S. Hoffman, *J. Biomed. Mater. Res.* **1990**, *24*, 21–38.
- [21] a) R. Garzon, G. A. Calin, C. M. Croce, *Annu. Rev. Med.* **2009**, *60*, 167–179; b) N. Yanaihara, N. Caplen, E. Bowman, M. Seike, K. Kumamoto, M. Yi, R. M. Stephens, A. Okamoto, J. Yokota, T. Tanaka, G. A. Calin, C. G. Liu, C. M. Croce, C. C. Harris, *Cancer Cell* **2006**, *9*, 189–198; c) X. Liu, L. F. Sempere, F. Galimberti, S. J. Freemantle, C. Black, K. H. Dragnev, Y. Ma, S. Fiering, V. Memoli, H. Li, J. DiRenzo, M. Korc, C. N. Cole, M. Bak, S. Kauppinen, E. Dmitrovsky, *Clin. Cancer Res.* **2009**, *15*, 1177–1183.